

Importance of the Initial Oxidation State of Copper for the Catalytic Hydrogenation of Dimethyl Oxalate to Ethylene Glycol

Yannan Sun,^[a, b] Fanqiong Meng,^[a] Qingjie Ge,^[a] and Jian Sun^{*[a]}

Exposing a Cu-based catalyst to a suitable temperature is of great importance to optimize its hydrogenation performance, as copper is sensitive to temperature. Herein, we investigated the effect of the initial oxidation state of copper, tuned by the reduction temperature, on its catalytic performance in the hydrogenation of dimethyl oxalate (DMO) to ethylene glycol (EG) through designing a series of catalysts with different reduction temperatures (200–350 °C). Among these catalysts, the Cu/SiO₂ catalyst prepared by ammonia evaporation with a hydrogen reduction process at 250 °C showed the best performance in the hydrogenation of DMO with a conversion of 100% and a selectivity to EG higher than 95%. The relationship between

the initial oxidation state of copper and catalytic performance was well established by characterizing the physicochemical properties of the Cu/SiO₂ catalysts by XRD, TEM, H₂ temperature-programmed reduction, N₂O adsorption, and in situ reduction Auger electron spectroscopy. The initial oxidation state of copper determined the conversion of DMO and the distribution of the products, and it could be balanced by reducing the temperature to improve the activity of the catalyst. This work provides a reference for further exploration of the mechanism and guidance for the design of catalysts for the hydrogenation of esters.

1. Introduction

Ethylene glycol (EG) is an important chemical intermediate that is applied broadly in industry. Various processes for the production of ethylene glycol have been used in industry, and the main process involves the use of fossil fuels, especially the use of ethylene oxide in a hydration reaction.^[1] Considering the shortage of oil, new synthetic approaches from syngas have come to the attention of researchers. This route includes the coupling of CO with methanol to give dimethyl oxalate (DMO) and the hydrogenation of DMO to produce EG.^[2]


However, the second hydrogenation step suffers from difficulties that remain to be solved, and the mechanism is still under discussion. There are numerous factors that influence the activity and selectivity of the reaction, including the method used to prepare starting materials, the loading of the


metal catalyst, and the liquid hourly space velocity (LHSV). Various methods for the preparation of the catalysts have been reported, including hydrolysis precipitation,^[3] deposition–precipitation,^[4] sol–gel,^[5] ammonia evaporation,^[6] and other new methods for different catalytic systems with enhanced activity. Han et al. reported Pd–Au–CuO_x prepared through the galvanic deposition of Pd and Au onto a thin-sheet, microfibrillar structure by using 8 mm Cu fibers, which synergistically promoted the hydrogenation activity and stabilized the Cu⁺ sites.^[7] Zhang et al. reported a plasma-treated Cu–Ni/ZrO₂ catalyst that had enhanced Cu dispersion.^[4]

Silica-supported copper catalysts have excellent performance and have widely been used in hydrogenation reactions because of their excellent performance.^[6c,8] SiO₂, as a kind of carrier, has been used in the preparation of catalysts, such as silica sol,^[9] tetraethyl orthosilicate (TEOS),^[6c] aerosil,^[10] and mesoporous silica.^[6c] Various dopants have also been used to modify the catalysts.^[11] Liu et al. designed a Ag–Cu–SiO₂ catalyst and discovered that the strong interaction between Cu and Ag benefitted the activity of the catalyst, which lasted up to 1100 h.^[10] Zhang et al. reported a Cu–Ni/ZrO₂ catalyst with high selectivity and stability.^[4] Furthermore, new methods and structures have been applied to enhance the performance of catalysts. Ye et al. used a dextrin coating on Cu–SiO₂ catalysts to obtain excellent stability and activity under conditions of a high weight liquid hour space velocity (WLHSV).^[9] Yao et al. reported a copper silicate nanoreactor with nanotube-assembled hollow spheres that maintained high selectivity and conversion even at a low H₂/DMO molar ratio of 20 in contrast with typical values of 80–200.^[12] Ye et al. reported a new metal–organic

[a] Y. Sun, F. Meng, Q. Ge, Dr. J. Sun
Dalian National Laboratory for Clean Energy
Dalian Institute of Chemical Physics, Chinese Academy of Sciences
457 Zhongshan Road, Dalian 116023 (China)
E-mail: sunj@dicp.ac.cn

[b] Y. Sun
School of Chemical Engineering
University of Chinese Academy of Sciences
380 Huaibeizhuang, Huaibei Town, Huairou District, Beijing 101408 (China)

 The ORCID identification number(s) for the author(s) of this article can be found under:
<https://doi.org/10.1002/open.201800225>.

 © 2018 The Authors. Published by Wiley-VCH Verlag GmbH & Co. KGaA. This is an open access article under the terms of the Creative Commons Attribution-NonCommercial License, which permits use, distribution and reproduction in any medium, provided the original work is properly cited and is not used for commercial purposes.

framework (MOF)-derived Cu/SiO₂ catalyst that achieved more than 95.0% selectivity to EG with a long lifetime of 220 h and a copper loading of only 7.83%.^[13]

For the Cu-SiO₂ catalytic system, before the reaction, the calcined copper catalysts were reduced under a hydrogen atmosphere, and in this section, the high valence of copper was reduced to Cu⁺ and Cu⁰, which may be the primary active sites for hydrogenation.^[2a,14] It is generally accepted that the synergy between Cu⁰ and Cu⁺ promotes the conversion of DMO and the selectivity to the products.^[15]

The effect of the initial oxidation state of copper after reduction under a hydrogen atmosphere on its catalytic performance in the hydrogenation of DMO to EG is still not clear. The reduction temperature is a vital factor that affects the properties of the reduced catalyst, as it influences the morphology, the oxidation state of the copper species, and the activity, because copper catalysts are sensitive to temperature. In this work, we designed a series of highly dispersed gaseous silica-supported Cu catalysts prepared by ammonia evaporation with different reduction temperature (200–350 °C) to disclose the relationship between the initial oxidation state of copper and catalytic performance. In combination with systematic characterization, the nature of copper after activation under different conditions was investigated and discussed in detail.

2. Results and Discussion

2.1. Catalytic Performance in the Hydrogenation of DMO

The catalytic performance of Cu/SiO₂ reduced at different temperatures is shown in Table 1 and Figure 1. The reaction temperature was initially 210 °C and was then decreased gradually until deactivation. The main products were methyl glycolate (MG) and ethylene glycol, as well as a small amount of ethanol (EO) at 180 °C. MG is the product of the first step of the hydrogenation,^[16] but the higher content of MG portends the deactivation of the catalyst.

At a reaction temperature of 180 °C, the catalyst reduced at 250 °C had an outstanding performance with a conversion of 100% and selectivity to EG of 95.2%. In addition, the catalysts reduced at 200 and 300 °C both showed conversions over 90% with selectivities to EG of 71.5 and 84.6%, respectively. The cat-

Reduction temperature [°C]	DMO conversion [%]	Product selectivity [%]		
		MG	EG	EO
unreduced	58.6	79.9	19.8	0.1
200	93.8	27.8	71.5	0.4
250	100.0	1.1	95.2	1.1
300	96.6	14.5	84.6	0.3
350	89.9	24.9	73.0	1.0

[a] Reaction conditions: 180 °C, 3.0 MPa, $n(\text{H}_2)/n(\text{DMO})=80$, LHSV = 0.5 h⁻¹.

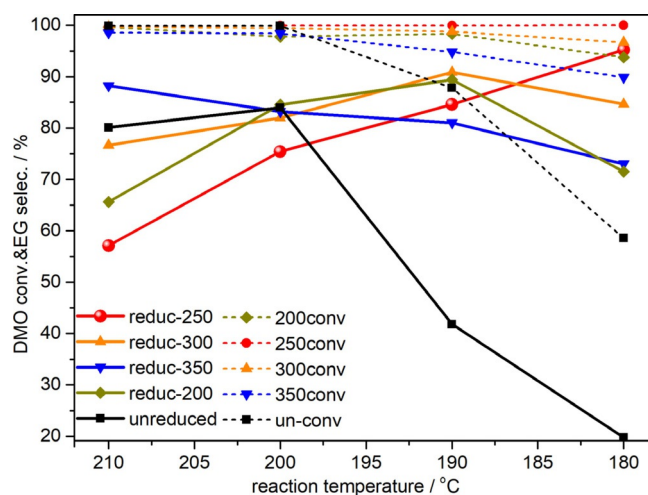


Figure 1. Conversion of DMO and selectivity to EG in the hydrogenation of DMO over various Cu/SiO₂ samples.

alyst reduced at 350 °C showed a DMO conversion slightly lower than 90% and a lower selectivity to EG of 73.0%.

Upon decreasing the reaction temperature, the conversion of DMO and the selectivity to EG decreased for the catalyst reduced at 350 °C; deactivation occurred below 200 °C, as the selectivity to MG was over 10% and the conversion of DMO was below 95%. On the contrary, for the catalyst reduced at 250 °C, the DMO conversion was maintained nearly at 100%, and at the same time, the selectivity to EG increased. However, upon decreasing the reaction temperature, the DMO conversions of the catalysts reduced at 200 and 300 °C slightly decreased but were still over 98% with a reaction temperature over 190 °C. Upon decreasing the reaction temperature to 180 °C, the DMO conversions of the catalysts decreased to 93.8 and 96.6%, respectively, and they both showed volcano-type curves for the selectivity to EG that peaked at around 190 °C. Deactivation of these two catalysts occurred below 190 °C with a marked increase in the selectivity to MG. The highest selectivities to EG for the catalysts reduced at 200, 250, 300, and 350 °C were 89.4, 95.2, 90.9, and 88.2%, respectively.

As a comparison, we measured the activity of Cu/SiO₂ that went through the same pretreatment temperature and time as the reduc-250 catalyst under a nitrogen atmosphere but without reduction under a hydrogen atmosphere (Figure 1). Most of the copper species in the unreduced catalysts were Cu²⁺; the Cu²⁺ species are not the active sites for the hydrogenation reaction, but in the reaction process, some Cu²⁺ might also be reduced to Cu⁺ and Cu⁰. The reduced copper species were not abundant, and as a result, the performance of the catalyst was unsatisfactory; furthermore, a volcano-type curve for the selectivity to EG was found.

2.2. Dispersion of Cu

Figure 2 shows the TEM images of the reduced Cu/SiO₂ samples prepared by the ammonia evaporation method at different reduction temperatures. It is clear that the copper particles

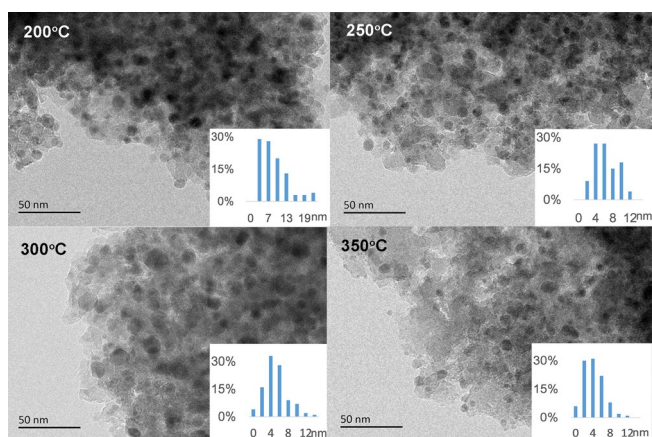


Figure 2. TEM images of Cu/SiO₂ reduced at 200, 250, 300, and 350 °C.

are highly dispersed. The observed catalysts were sensitive to the electron beam and the silica moved fast. We chose the edges of the big agglomerate pieces formed under the electron beam for more distinct observation. From the images, it can be seen that the silica is amorphous and that the copper particles are well dispersed, dark, small, and have a nearly round shape.

Good dispersion of the Cu nanoparticles was caused by the formation of copper phyllosilicate during the preparation process. As reported, copper phyllosilicate [Cu₂Si₂O₅(OH)₂] is a kind of copper silicate with a lamellar structure that has a high specific surface area that can disperse copper species well, and the Cu species in copper phyllosilicate have an oxidation state of +2.^[11c] The average particle sizes (Table 2 and Figure 2) were determined on the basis of the statistics of the copper particles. The average particle size of copper reduced at 200 °C was larger than that of the other three catalysts, the particle sizes of which had not conspicuous differences. The reduction temperature affected the particle size, and the reason may be that the copper particles are sensitive to temperature and low temperatures make the copper particles diminish in size. However, if the reduction temperature was over 250 °C, the copper particles were well reduced and formed a balance of Cu⁰ and Cu⁺ sites, which were well dispersed. Consequently, these particle sizes are smaller than those for the catalyst reduced at

Reduction temperature [°C]	S _{BET} [m ² g ⁻¹]	V _p [cm ³ g ⁻¹]	d _{Cu1} ^[b] [nm]	d _{Cu2} ^[c] [nm]
SiO ₂ unreduced	226	0.55	N.A.	N.A.
200	370	0.56	N.A.	N.A.
250	230	0.54	10.2	3.9
300	205	0.53	7.3	3.1
350	201	0.52	8.1	3.7
350	204	0.52	7.2	3.4

[a] S_{BET}: BET surface area of the catalysts and the carrier, V_p: total pore volume of the catalysts and the carrier. [b] Cu particle size determined from the TEM images. [c] Cu particle size calculated by the Scherrer equation.

250 °C. Another possibility is that the copper species were not reduced well at 200 °C, as this would result in differences in the physical and chemical properties of the catalysts.

2.3. XRD Patterns

The X-ray diffraction patterns are summarized in Figure 3. The peak at about 2θ = 21.7° belongs to amorphous silica.^[17] The broad diffraction peaks at 2θ = 31.2, 35.8, 57.3, and 63.2° suggest the presence of copper phyllosilicate in the unreduced catalyst.^[17] The diffraction peaks are very diffuse, which shows

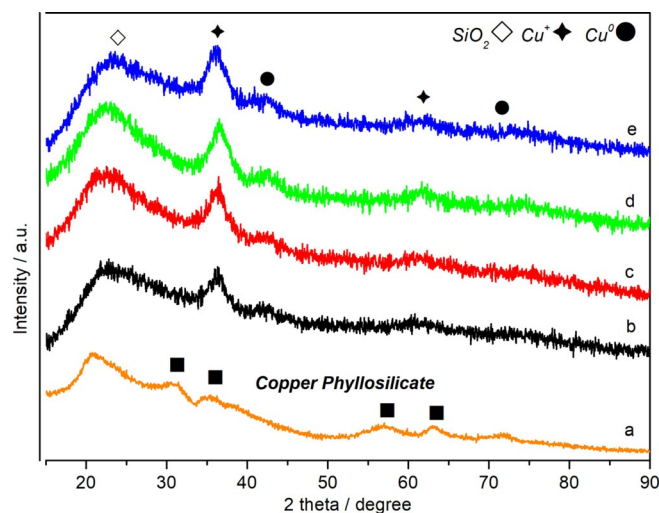


Figure 3. XRD patterns of Cu/SiO₂ samples a) unreduced, b) reduced at 200 °C, c) reduced at 250 °C, d) reduced at 300 °C, and e) reduced at 350 °C.

that Cu species are finely dispersed onto the silica supports. In the patterns of the reduced samples, the peaks for copper phyllosilicate cannot be observed and peaks appear for Cu⁺ at 2θ = 36.4 and 61.5° (JCPDS 065-3288) and for Cu⁰ at 2θ = 43.3 and 74.1° (JCPDS 004-0836). The copper particle sizes in these catalysts were calculated by the Scherrer formula by using the full width at half maximum (FWHM) of the Cu⁺ diffraction peak at 2θ = 36.6° and are listed in Table 2. The particle sizes range from 3 to 4 nm, and the differences are not apparent.

During the preparation of the Cu/SiO₂ catalysts by the ammonia evaporation (AE) method, copper phyllosilicate, which is stable, is generated. Then, copper phyllosilicate is reduced to Cu⁰ and Cu⁺, so that the copper species on the catalysts prepared by the AE method are well dispersed and have an even particle-size distribution.

Combined with similar results obtained from the XRD patterns and TEM images, the reduction temperature has little impact on the particle size of the copper species. Therefore, the particle size is not the primary factor determining the performance of the catalysts in the hydrogenation of DMO in the reduction temperature range of 250 to 350 °C.

2.4. Stability of the Catalysts

Figure 4 shows the stability of the reduc-250 catalyst; it shows a stable trend with a time on stream of 16 h. The conversion of DMO is maintained near 100%, whereas the selectivity to EG gradually climbs from 90 to 95% within the first 6 h and remains stable after the next 10 h. To investigate possible coke on the used catalyst, the temperature-programmed oxidation (TPO) mass spectrum is shown in Figure 5. The Cu/SiO₂ catalyst exhibits CO₂ release at 200–300 and 400–600 °C that is accompanied by water release over a wider temperature range, which suggests possible adsorption of carbon species on the catalyst surface. These carbon species probably originate from alcohol products adsorbed on the active sites after the long reaction time. In addition, the XRD pattern of the used catalyst (Figure 6) shows that copper mainly exists in form of Cu⁺, which results from oxidation of a fraction of metallic copper during the reaction.

The XRD pattern of the used unreduced Cu/SiO₂ catalyst is shown in Figure 6. It shows the coexistence of Cu⁺ and Cu⁰. This result implies that the reduction of copper phyllosilicate proceeds during in situ DMO hydrogenation by H₂. However, the conversion of DMO is lower than that on other reduced cata-

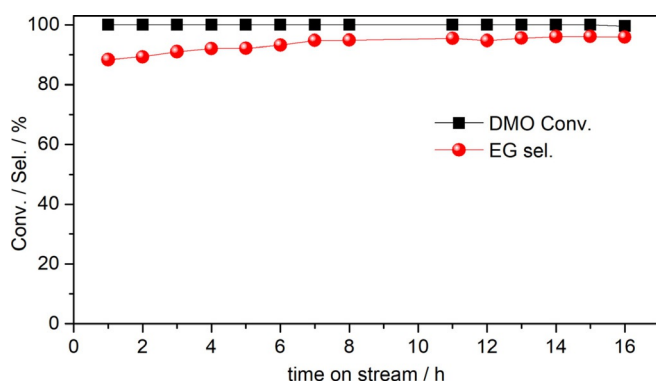


Figure 4. Stability of the reduc-250 catalyst in the hydrogenation of DMO. Reaction conditions: 180 °C, 3.0 MPa, $n(\text{H}_2)/n(\text{DMO})=80$, LHSV = 0.5 h⁻¹.

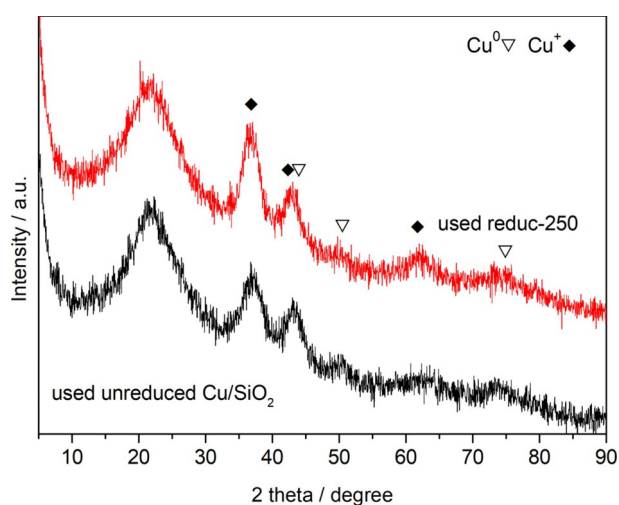


Figure 5. XRD pattern of the used, unreduced Cu/SiO₂ catalyst.

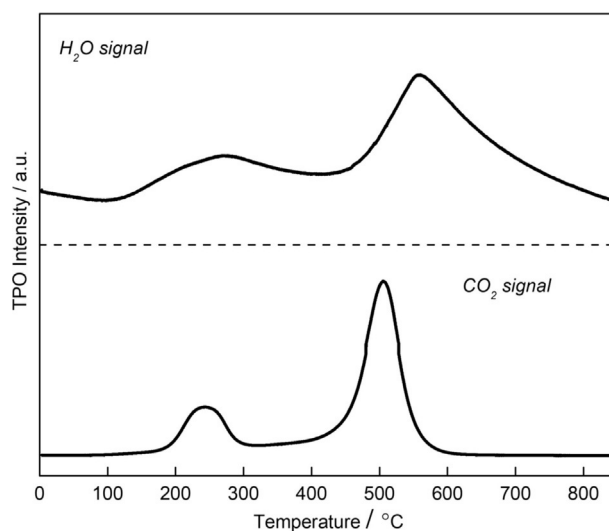


Figure 6. TPO-MS spectra after stability.

lysts, as not enough Cu⁰ is provided in the initial stage (Figure 3). The selectivity to EG reaches a maximum at a temperature of 200 °C, which is higher than that for the reduced catalysts (190–180 °C). Deactivation occurs below 200 °C, which results in a high selectivity to MG at a low temperature of 180 °C.

2.5. Physicochemical Properties

The specific surface areas and pore volumes calculated from the N₂ adsorption–desorption isotherms of the samples are shown in Table 2. The reason that the surface area increases after the copper species are loaded onto the silica can be attributed to the formation of copper phyllosilicate, which has a lamellar structure and a high specific surface area.^[2a] Upon reduction of copper phyllosilicate, the structure might be destroyed, and thus, the surface area decreases. The Cu/SiO₂ sample reduced at 200 °C has a larger surface area than the samples reduced at higher temperatures, and this may indicate that copper phyllosilicate is not reduced completely. All of these catalysts and the support have comparable pore volumes, which indicates that a reduction in the temperature does not significantly affect the pore volume.

Several characterization methods were used to confirm the differences in the physical properties of the catalysts reduced at different temperatures. Copper species were not reduced entirely at 200 °C, and a certain amount of copper phyllosilicate might still remain. Copper species were well reduced over 250 °C, and the three samples reduced at 250, 300, and 350 °C were similar to each other in terms of special surface area, dispersity, pore volume, and particle size.

2.6. H₂ Temperature-Programmed Reduction and N₂O Adsorption Profiles of the Catalysts

The catalysts reduced at different temperatures showed similar physical properties; thus, we predicted that there were crucial

chemical properties that determined the catalytic activities. Further characterization was undertaken to explore the origin of the Cu/SiO₂ catalysts with different initial oxidation states after reduction with different temperatures. A temperature-programmed reduction (TPR) signal for the Cu/SiO₂ catalysts was first recorded at a ramping rate of 10 °C min⁻¹ until the specified reduction temperature, and subsequently, a constant temperature was maintained for 2 h.

As shown by the black line in Figure 7a, the copper species were reduced slowly for a long time at 200 °C but were probably still not entirely reduced. As the temperature increased, Cu species with a reduction temperature over 250 °C were well reduced and displayed a similar sharp reduction peak centered at 250 °C. The TPR curves terminated at 300 and 350 °C indicate a peak reduction temperature of 250 °C. A higher reduction temperature contributed to deeper reduction. In this catalyst system, a temperature over 250 °C was a proper condition that could reduce the copper species well. The catalyst was

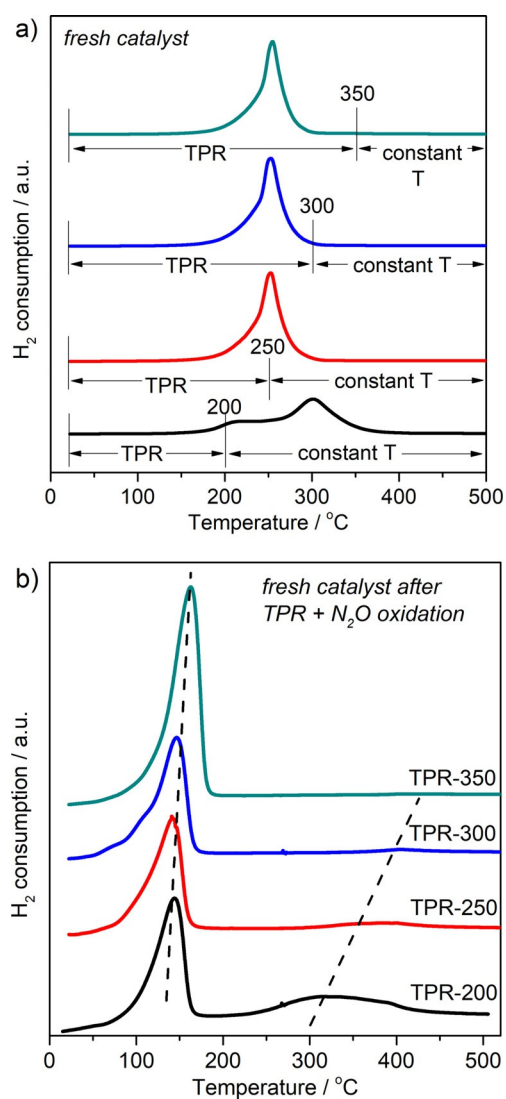


Figure 7. TPR profiles of the Cu/SiO₂ samples: a) TPR profiles of the fresh catalysts and b) the second TPR profiles after TPR and N₂O adsorption.

not completely reduced at 200 °C, and this is consistent with the results of previous analyses.

After H₂-TPR, N₂O was in situ introduced and adsorbed on the catalyst surface to react with metallic copper. In this process, the exposed Cu⁰ species on the surface were further oxidized to Cu⁺, and then a second H₂-TPR process was terminated at a temperature higher than 500 °C (Figure 7b). The Cu⁺ formed during N₂O oxidation can be easily reduced at a low temperature with a H₂ consumption peak at 130–150 °C. Furthermore, there is a remarkably broad peak centered at about 330 °C in the reduction curve of the catalyst reduced at 200 °C and the peaks are much smaller to nearly nonexistent in the curves of the catalysts reduced at 250, 300, and 350 °C. The peak shows that there might be copper species that are not reduced to Cu⁰ in the first reduction process. Therefore, in the second reduction process, another peak different from the reduction peak of Cu⁺ oxidized by N₂O is observed.

In addition, as the reduction temperature increases, the first main TPR peaks and the peaks at higher temperatures after N₂O adsorption shift towards higher temperatures; this is caused by a strong interaction between the copper species and silica.^[3] Accordingly, it can be predicted that higher reduction temperatures induce stronger interactions of the metal and the carrier, which consequently influences the hydrogenation performance of the catalysts.

2.7. In Situ Reduction Auger Electron Spectroscopy

The identification of the Cu species in the reduced catalyst is based on ex situ characterization by XRD, TEM, and BET analysis and also on many previous works. To investigate the real oxidation state of copper after reduction, the in situ reduction Auger electron spectroscopy (AES) results are summarized in Figure 8 and Table 3 to show the surface compositions and chemical states of the reduced Cu/SiO₂ catalysts. The two overlapping peaks of Cu⁺ and Cu⁰ at 914.3 and 918.2 eV are separated.^[11d,18] The ratio of surface Cu⁺ decreases as the reduction increases. The ratio of Cu⁺ in the catalyst reduced at 200 °C is 0.41, and the ratio of Cu⁺ in the catalyst reduced at 250 °C is 0.41, which is slightly lower than that in the catalyst reduced at 200 °C. The ratios in the catalysts reduced at 300 and 350 °C are clearly lower than those in the catalysts reduced at 200 and 250 °C.

As reported, Cu⁰ is reduced from CuO and Cu⁺ is reduced from copper phyllosilicate. As CuO has a weak interaction with SiO₂, it can be easily reduced to Cu⁰. However, there is a strong interaction between Cu and Si in copper phyllosilicate, and this interaction can stabilize Cu⁺ as a final state without further reduction to Cu⁰. However, exposure of the catalyst to a higher reduction temperature affects the structure of copper phyllosilicate and, thus, the interaction of the Cu–O bond, which leads to deeper reduction and the production of a larger amount of Cu⁰. Therefore, the temperature plays an important role in balancing the ratio of Cu⁺ and Cu⁰.

It has been suggested that Cu⁰ species are the active sites and the main elements for activation of H₂, whereas Cu⁺ species promote the conversion of intermediates.^[2b] Cu⁰ facilitates

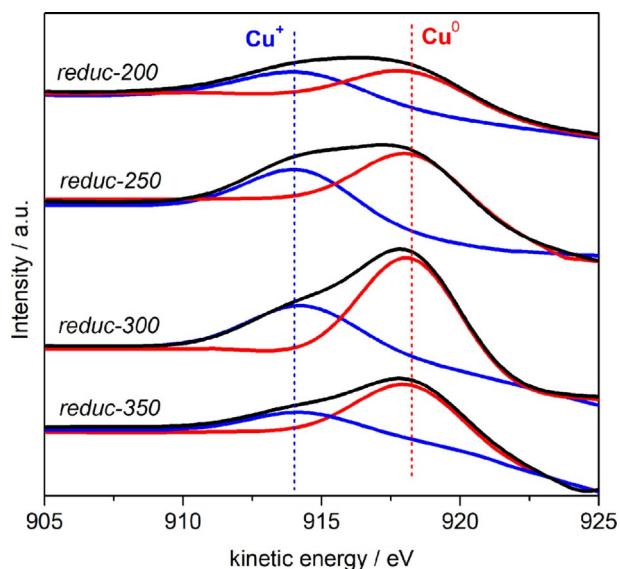


Figure 8. In situ AES results of the Cu/SiO₂ catalysts after reduction at various temperatures.

Reduction temperature [°C]	Kinetic energy [eV]		Cu ⁺ /(Cu ⁺ + Cu ⁰)
	Cu ⁺	Cu ⁰	
200	914.3	918.2	0.41
250	914.3	918.2	0.40
300	914.3	918.2	0.27
350	914.3	918.2	0.24

the decomposition of H₂, and Cu⁺ adsorbs methoxy and acyl species. Therefore, the ratio of Cu⁺ and Cu⁰ determines the conversion of DMO and the distribution of the products. Balancing the ratio of Cu⁺ and Cu⁰ is of great importance.^[19] If copper species are not reduced entirely, the active sites will be not abundant for the hydrogenation of DMO. However, if the reduction temperature is too high, the copper species will produce a stronger interaction with the silica support, which finally affects the selectivity to EG.^[3] Thus, it is difficult for the intermediate products to be transformed into EG. It can be concluded that a balanced initial Cu⁰/Cu⁺ state achieved by a suitable reduction temperature is the key to control the performance of catalysts in the hydrogenation of DMO to EG (as described in Figure 9).

In addition, there are many Cu/SiO₂ catalytic systems for which different kinds of SiO₂ sources are employed, and therefore, the selected reduction temperatures for activating Cu are not the same, such as silica sol^[9] (350 °C), TEOS^[6c] (350 °C), aerosol^[10] (250 °C), and mesoporous silica^[6c] (300 °C). This probably depends on the degree of interaction between the copper particles and the different kinds of silica. Kinetic elements determine the best reduction temperature in different Cu/SiO₂ systems. The aerosol-supported copper catalyst reduced at 250 °C has an appropriate ratio of Cu⁺ as well as an abundance of reduced copper species, and as a result, it exhibits the highest

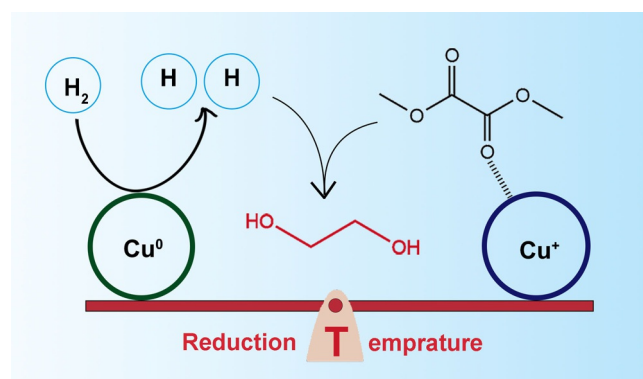


Figure 9. Schematic for the hydrogenation of DMO to EG controlled by the initial oxidation state of copper.

selectivity to EG as well as the stable and high conversion of DMO.

In addition to the Cu⁺/Cu⁰ ratio, the specific area of Cu and the dispersion of Cu are other factors that affect the hydrogenation performance of Cu. Herein, we compared these properties. The data suggest that the dispersion of Cu and the specific area of Cu are different for the catalysts reduced at different temperatures (Table 4). The reduc-200 catalyst shows the lowest Cu dispersion and the lowest Cu specific area, as reduction of Cu is incomplete and not enough Cu is exposed on the surface. However, after reduction with a temperature higher than 250 °C, the specific area of Cu remains almost unchanged owing to a complete reduction process. Upon comparing reduc-200 and reduc-250, the primary factor affecting the hydrogenation performance lies in the exposed active Cu specific area, despite similar Cu⁺/Cu⁰ ratios.

Catalyst	Cu dispersion [%]	Specific area of Cu [m ² g ⁻¹]
reduc-200	23.7	160.1
reduc-250	29.4	198.6
reduc-300	30.9	208.9
reduc-350	29.7	200.6

3. Conclusions

In light of the above, the initial oxidation state of copper before the reaction significantly influences the hydrogenation performance of Cu-based catalysts. In detail, a significant factor determined by the reduction temperature is the Cu⁺/Cu⁰ ratio. Lower temperatures cannot reduce the copper species entirely, whereas higher temperatures may lead to inappropriate Cu⁰/Cu⁺ ratios and a stronger interaction between copper and silica. An appropriate reduction temperature can produce a catalyst with a balance of Cu⁰ and Cu⁺ sites and other properties to attain better catalytic performance. However, the reduction temperature has very little effect on the particle size of Cu, crystalline phase, BET surface area, and pore

properties. A Cu-aerosol catalyst reduced at 250 °C exhibits the stable and high conversion of DMO and the highest selectivity to EG contrasting with the catalysts reduced at other temperature. This work established the relationship between the initial oxidation state of copper and the activity of the catalyst to provide a reference for further exploration of the mechanism and guidance for the design of hydrogenation catalysts.

Experimental Section

Catalyst Preparation

The Cu/SiO₂ catalyst was prepared by the ammonia evaporation (AE) method. Cu(NO₃)₂·3H₂O (15.2 g, Tianjin Kermel Corp) was dissolved in deionized water (210 mL), and an aqueous solution of ≈25–28% ammonia (21 mL, Tianjin Kermel Corp) was added under agitation. Then, aerosil (16 g, Evonik Degussa A300) was added into the solution. After stirring at 40 °C for 4 h, the temperature was increased to 90 °C to evaporate ammonia and to deposit the copper species onto the silica. The pH value of the suspension decreased to roughly 7–8 over about 2 h, and the evaporation procedure was terminated. The precipitate was washed with deionized water until its conductivity was under 100 Ω⁻¹. The sample was dried at 120 °C for 12 h and was then calcined at 450 °C for 4 h. Before the reaction, the catalyst was pelletized, crushed, and sieved to 20–40 mesh.

Catalyst Activity Test

The performance of the catalyst was tested in a continuous-flow fixed-bed reactor. The catalyst (1 g) was packed into a stainless-steel tubular reactor (internal diameter of 12 mm) with a thermocouple inserted into the catalyst bed. Before the reaction, the catalyst was reduced at 200, 250, 300, or 350 °C for 4 h under an atmosphere of pure hydrogen with a ramping rate of 1 °C min⁻¹ or was reduced at 250 °C under nitrogen flow as a comparison. Dimethyl oxalate (Acros Organics) dissolved in methanol (Tianjin Kermel Corp) was injected into the vaporizer by metering pumps, heated, and then introduced into the reactor, mixing with H₂. The gaseous products were cooled down in the cold trap and were analyzed by a Varian CP 3800 gas chromatograph with a flame ionization detector (FID).

XRD

The X-ray diffraction (XRD) patterns were collected with an X'Pert PRO diffractometer (PANalytical) by using CuKα radiation of 40 kV and 40 mA. The scanning angles ranged from 6 to 90°. The powder catalyst sample was shaped into a glass plate with a width of 13 mm and a thickness of 1.5 mm before measurements.

N₂ Adsorption

Nitrogen adsorption-desorption isotherms were conducted by static N₂ adsorption at -196 °C with a Quantachrome (Quadrasorb SI) analyzer. The samples were outgassed at a temperature of 120 °C for 1 h and were evacuated at 300 °C for 3 h to remove impurities adsorbed physically. The surface area was calculated by the Brunauer-Emmett-Teller (BET) method. The total pore volume (V_p) was measured by the adsorbed N₂ volume at a relative pressure of about 0.98.

TEM

Transmission electron microscopy (TEM) images were obtained with a JEM-2100 transmission electron microscope operating at an acceleration voltage of 300 kV. The catalyst powder was ultrasonically dispersed in ethanol at room temperature for 30 min and was transferred onto a carbon-coated copper or nickel grid by dipping before measuring.

H₂-TPR, TPO, and N₂O Adsorption

Temperature-programmed reduction (TPR) was performed by using a homemade apparatus. The Cu/SiO₂ sample (25 mg) was put into a quartz U-type tubular reactor and was outgassed at 300 °C under an argon atmosphere for 40 min. After cooling to room temperature, the sample was heated to a specified temperature at a ramping rate of 10 K min⁻¹ in a 5% H₂/95% argon gas mixture. Temperature-programmed oxidation (TPO) was similar to TPR; after the catalyst was outgassed, the sample was programmed heated to 800 °C in an O₂/He gas mixture.

After cooling to room temperature again, N₂O adsorption was performed. 15% N₂O/He was introduced for 1 h to oxidize surface Cu⁰ to Cu₂O. Then, Cu₂O oxidized by N₂O was reduced again by hydrogen. The consumptions of H₂ and N₂O were monitored by using a thermal conductivity detector (TCD). The Cu dispersion and the specific area of Cu were calculated from N₂O adsorption.^[20]

In Situ Reduction AES

In situ Auger electron spectroscopy (AES) was performed with a spectrometer (ULVAC-PHI, Japan) with an Mg Kα X-ray source (E = 1253.6 eV). Before measurements, the catalysts were tableted and reduced in pure hydrogen flow at the specified temperature (200, 250, 300, or 350 °C) for 2 h in the pretreatment room, and then the catalysts were shifted to the chamber to be outgassed and measured.

Acknowledgements

The authors are thankful for support of the Hundred-Talent Program of Dalian Institute of Chemical Physics, the Youth Innovation Promotion Association of Chinese Academy of Sciences (2018214), and the National Natural Science Foundation of China (21466030).

Conflict of Interest

The authors declare no conflict of interest.

Keywords: copper • esters • hydrogenation • oxidation state • reduction

- [1] H. Yue, Y. Zhao, X. Ma, J. Gong, *Chem. Soc. Rev.* **2012**, *41*, 4218–4244.
- [2] a) J. Gong, H. Yue, Y. Zhao, S. Zhao, L. Zhao, J. Lv, S. Wang, X. Ma, *J. Am. Chem. Soc.* **2012**, *134*, 13922–13925; b) H. Yue, X. Ma, J. Gong, *Acc. Chem. Res.* **2014**, *47*, 1483–1492.
- [3] Y. Zhao, S. Li, Y. Wang, B. Shan, J. Zhang, S. Wang, X. Ma, *Chem. Eng. J.* **2017**, *313*, 759–768.
- [4] C. Zhang, D. Wang, M. Zhu, F. Yu, B. Dai, *Catal. Commun.* **2017**, *102*, 31–34.

- [5] A. Yin, X. Guo, W.-L. Dai, K. Fan, *J. Phys. Chem. C* **2009**, *113*, 11003–11013.
- [6] a) X. Kong, C. Ma, J. Zhang, J. Sun, J. Chen, K. Liu, *Appl. Catal. A* **2016**, *509*, 153–160; b) B. Wang, Y. Cui, C. Wen, X. Chen, Y. Dong, W.-L. Dai, *Appl. Catal. A* **2016**, *509*, 66–74; c) Y. Zhao, Y. Zhang, Y. Wang, J. Zhang, Y. Xu, S. Wang, X. Ma, *Appl. Catal. A* **2017**, *539*, 59–69; d) A. Yin, X. Guo, W. L. Dai, K. Fan, *Catal. Commun.* **2011**, *12*, 412–416.
- [7] L. Han, L. Zhang, G. Zhao, Y. Chen, Q. Zhang, R. Chai, Y. Liu, Y. Lu, *ChemCatChem* **2016**, *8*, 1065–1073.
- [8] R.-P. Ye, L. Lin, Q. Li, Z. Zhou, T. Wang, C. K. Russell, H. Adidharma, Z. Xu, Y.-G. Yao, M. Fan, *Catal. Sci. Technol.* **2018**, *8*, 3428–3449.
- [9] R.-P. Ye, L. Lin, J.-X. Yang, M.-L. Sun, F. Li, B. Li, Y.-G. Yao, *J. Catal.* **2017**, *350*, 122–132.
- [10] Y. Liu, J. Ding, J. Yang, J. Bi, K. Liu, J. Chen, *Catal. Commun.* **2017**, *98*, 43–46.
- [11] a) P. Ai, M. Tan, N. Yamane, G. Liu, R. Fan, G. Yang, Y. Yoneyama, R. Yang, N. Tsubaki, *Chem. Eur. J.* **2017**, *23*, 8252–8261; b) Z. He, H. Lin, P. He, Y. Yuan, *J. Catal.* **2011**, *277*, 54–63; c) S. Zhao, H. Yue, Y. Zhao, B. Wang, Y. Geng, J. Lv, S. Wang, J. Gong, X. Ma, *J. Catal.* **2013**, *297*, 142–150; d) X. Zheng, H. Lin, J. Zheng, X. Duan, Y. Yuan, *ACS Catal.* **2013**, *3*, 2738–2749; e) A. Yin, C. Wen, X. Guo, W.-L. Dai, K. Fan, *J. Catal.* **2011**, *280*, 77–88; f) L. Han, G. Zhao, Y. Chen, J. Zhu, P. Chen, Y. Liu, Y. Lu, *Catal. Sci. Technol.* **2016**, *6*, 7024–7028.
- [12] D. Yao, Y. Wang, Y. Li, Y. Zhao, J. Lv, X. Ma, *ACS Catal.* **2018**, *8*, 1218–1226.
- [13] R.-P. Ye, L. Lin, C.-C. Chen, J.-X. Yang, F. Li, X. Zhang, D.-J. Li, Y.-Y. Qin, Z. Zhou, Y.-G. Yao, *ACS Catal.* **2018**, *8*, 3382–3394.
- [14] J. Y. Kim, J. A. Rodriguez, J. C. Hanson, A. I. Frenkel, P. L. Lee, *J. Am. Chem. Soc.* **2003**, *125*, 10684–10692.
- [15] S. Li, Y. Wang, J. Zhang, S. Wang, Y. Xu, Y. Zhao, X. Ma, *Ind. Eng. Chem. Res.* **2015**, *54*, 1243–1250.
- [16] H. Yue, Y. Zhao, S. Zhao, B. Wang, X. Ma, J. Gong, *Nat. Commun.* **2013**, *4*, 2339.
- [17] X. Dong, X. Ma, H. Xu, Q. Ge, *Catal. Sci. Technol.* **2016**, *6*, 4151–4158.
- [18] a) L.-F. Chen, P.-J. Guo, M.-H. Qiao, S.-R. Yan, H.-X. Li, W. Shen, H.-L. Xu, K.-N. Fan, *J. Catal.* **2008**, *257*, 172–180; b) Y. Cui, B. Wang, C. Wen, X. Chen, W.-L. Dai, *ChemCatChem* **2016**, *8*, 527–531.
- [19] Y. Wang, Y. Shen, Y. Zhao, J. Lv, S. Wang, X. Ma, *ACS Catal.* **2015**, *5*, 6200–6208.
- [20] Z. Yuan, L. Wang, J. Wang, S. Xia, P. Chen, Z. Hou, X. Zheng, *Appl. Catal. B* **2011**, *101*, 431–440.

Received: October 23, 2018